Copy 213
RM A55D08

[redacted]

NACA RM A55D08

TECH LIBRARY KAFB, NM
0143366

8779
6448

RESEARCH MEMORANDUM

EXPERIMENTAL INVESTIGATION OF SOME AERODYNAMIC EFFECTS OF A GAP BETWEEN WING AND BODY OF A MODERATELY SLENDER WING-BODY COMBINATION AT A MACH NUMBER OF 1.4

By Duane W. Dugan

Ames Aeronautical Laboratory
Moffett Field, Calif.

(CLASSIFICATION CHANGED TO Unclassified)
NASA Tech Pub Announcement #8
(OFFICER AUTHORIZED TO CHANGE)
By ..... 26 Aug. 59
NK
(GRADE OF OFFICER MAKING CHANGE)
9 Mar. 61
DATE

CLASSIFIED DOCUMENT

This material contains information affecting the National Defense of the United States within the meaning of the espionage laws, Title 18, U.S.C., Secs. 793 and 794, the transmission or revelation of which in any manner to an unauthorized person is prohibited by law.

NATIONAL ADVISORY COMMITTEE FOR AERONAUTICS

WASHINGTON

May 27, 1955

[redacted]

[redacted]

B

 [redacted]

TECH LIBRARY KAFB, NM
0143366

NATIONAL ADVISORY COMMITTEE FOR AERONAUTICS

RESEARCH MEMORANDUM

EXPERIMENTAL INVESTIGATION OF SOME AERODYNAMIC EFFECTS OF A GAP BETWEEN WING AND BODY OF A MODERATELY SLENDER WING-BODY COMBINATION AT A MACH NUMBER OF 1.4

By Duane W. Dugan

SUMMARY

The effects of streamwise gaps between wing and body upon the lift and pitching moments of a moderately slender wing-body combination at a Mach number of 1.4 are experimentally determined and compared with available theoretical results. The investigation includes tests in which the angle of attack is varied with the all-movable wing at zero deflection and also tests in which the angle of wing deflection is varied with the body at zero angle of attack.

Results of the investigation show that the large losses in lift due to gap effects predicted by theory are realized only for angles of attack or of wing deflection near zero and for gap widths larger than 5 percent of the wing semispan. The percent losses in lift at all gap widths tend to diminish as the magnitude of the angle of attack or of wing deflection is increased, and for gap widths less than 1 percent of the wing semispan are very small except at angles near zero.

The effect of streamwise gaps upon the chordwise position of the center of pressure of the deflected wing is to cause it to move rearward for small gap widths and forward with wider gaps. A corresponding effect occurs with respect to the center of pressure of the body in the case of wing deflection.

INTRODUCTION

The use of all-movable wings hinged to the body in missile design has posed the problem of the nature and extent of the aerodynamic effects of the gaps associated with such an arrangement. In addition to the clearance required for mechanical reasons, a chordwise-varying gap between wing panels and curved fuselage is created by the deflection of the wing.

It has long been known that for subsonic incompressible flow, theory predicts that even the most minute streamwise gap in the middle part of a wing results in a relatively large loss in lift and a corresponding

[redacted]

increase in drag (e.g., ref. 1). More recently, effects of gaps upon the lift of slender wing-body combinations at supersonic speeds have been obtained theoretically. For example, Mirels (ref. 2) obtained a result for the case of a slender wing-body combination at angle of attack and with a gap between wing panels and cylindrical body; in addition, he gave an approximation for the effect of a chordwise-constant gap in the case of the same configuration but with the body at zero angle of attack and the wing deflected. In reference 3 the effects of a gap upon lift were obtained for a slender wing-body combination and its component parts for the cases of both angle of attack and of wing deflection. A method for estimating the effects of streamwise gaps on a number of aerodynamic characteristics of low-aspect-ratio wings at supersonic speeds, based on the replacement of a body by a perfect reflecting plane, was given in reference 4. In each of these theoretical investigations, based as they were on the assumption of an ideal fluid, the presence of an infinitesimally small gap was shown to result in considerable loss of lift.

To the writer's knowledge, little experimental investigation of the effects of streamwise gaps has been done. An early experiment at low subsonic speeds with a wing of rectangular plan form having a gap in the middle (ref. 5) indicated that significant losses in lift and increases in drag occurred for angles of attack near those for zero lift with gap widths only a few percent of the chord, but that these effects were reduced at higher angles. Reference 6 includes data obtained at supersonic speed for an all-movable wing-body combination having two small gap widths (0.0057 and 0.0220 wing semispan). As nearly as could be determined from the data presented, 6-percent loss in lift resulted from widening the gap when the angle of attack was varied 5° either side of zero and the wing was undeflected. Again, little or no effects of increasing the gap could be observed at large angles of attack or of wing deflection. Reference 7 contains pressure data at a Mach number of 1.9 for a wing and body simulator plate having gaps up to 0.50 inch (0.143 of wing semispan) between wing and plate. Briefly, the results indicated that for low values of lifting pressures the gap effects upon pressures were large with respect to the wing but slight with respect to the body simulator plate, and vice versa for larger lifting pressures.

Since the theories referred to above cannot be trusted to be valid in the range of very small gap widths nor for other than small angles, and because the available experimental data are inadequate, a detailed exploration of the aerodynamic effects of streamwise gaps characteristic of aircraft employing all-movable wings appears desirable. The present investigation was conducted in the Ames 6- by 6-foot supersonic wind tunnel at a Mach number of 1.4 and at a Reynolds number of approximately 2 million per foot with a test model comprised of a pointed cylindrical body and a low-aspect-ratio triangular wing, the two panels of which were individually supported at various gap distances from the body. The tests were conducted with the body and wing both at angle of attack, and with the body at zero angle of attack and the wing deflected. Results for the

effects of gap on lift and pitching moments of the wing-body combination and its component parts are presented in graphical form and compared with pertinent theoretical calculations.

NOTATION

Pertinent symbols and their meanings as used in this report are given below:

c maximum chord of each wing panel, in.

g width of gap between body and wing panel, measured along the hinge line, in.

p local static pressure, lb/sq ft

p_w reference wall pressure, lb/sq ft

q dynamic pressure of free stream, $\frac{1}{2}\rho V^2$, lb/sq ft

s semispan of wing-body combination when no gap exists, in.

x_{cp} chordwise distance from apex of wing panel to center of pressure, in.

H hinge moment of wing, lb-in.

M pitching moment about the hinge line, lb-in.

S area of wing formed by joining both wing panels, sq ft

V velocity of free stream, ft/sec

Z normal force, lb

C_h coefficient of hinge moment, $\frac{H}{qSc}$

C_m coefficient of pitching moment, $\frac{M}{qSc}$

C_p coefficient of pressure, $\frac{p-p_w}{q}$

C_Z coefficient of normal force, $\frac{Z}{qS}$

α angle of attack of body axis, deg

δ angle of wing deflection (angle between chord plane of wing and body axis), deg

ρ mass density of free [redacted]

APPARATUS

The experimental investigation was conducted in the Ames 6- by 6-foot wind tunnel. In this wind tunnel the Mach number can be varied continuously and the stagnation pressure can be varied to maintain a given test Reynolds number. A description of this facility may be found in reference 8.

Figure 1 shows a photograph of the test model, all parts of which are made of steel. The cylindrical body has a modified ogival nose section. The two right-triangular wing panels are supported independently with respect to the body in a midwing position along the constant-radius section of the body. The two beams supporting the wing panels are articulated 1/2 inch aft of the trailing edge to permit deflection of the panels with respect to the body. In order to simulate rotation about a fixed hinge line, translation of the wing panels was provided by the use of clamping blocks having correct dimensions for each angle of deflection. The wing panels can be set at any gap distance up to 9 inches from the body by means of an arrangement of motor-driven lead screws and carriages. A counter geared to the motor shaft enabled the setting of the gap from outside the tunnel test section.

Normal forces and pitching moments on the complete body including the section upstream of the apexes of the undeflected wing panels (hereafter designated "nose") and the section aft of the trailing edges of the wing panels (termed "afterbody") were obtained from the strain-gage balance on which the body was mounted in the wind tunnel. In addition, pressure measurements were obtained through the connection of pressure orifices in the body (see fig. 2) to a multiple-tube manometer employing tetrabromoethylene (sp. gr. 2.96 at 70° F) as a fluid and having its common sump vented to a reference wall pressure just upstream of the model.

Strain gages affixed to the beams supporting the wing panels enabled the measurement of bending moments at two streamwise stations from which normal forces and the streamwise location of the centers of pressures could be calculated as explained in the following section.

Further details of the model are summarized below or shown in figures 1 and 2.

Body

Fineness ratio, length/diameter	12.47
Over-all length, in.	44.88
Distance from nose tip to:	
End of ogival nose section (beginning of constant section), in.	22.50
Apex of wing panels (at zero deflection), in.	24.60
Trailing edge of wing panels (at zero deflection), in.	35.90
Imaginary hinge line of wing panels, in.	32.13
Diameter of constant section, in.	3.60

Wing panels	
Airfoil section	symmetric double wedge
Thickness (percent local chord)	5.0
Location of maximum thickness (percent local chord)	62.0
Maximum (root) chord, in.	11.30
Sweepback angle of leading edge, deg	60.0
Area, each panel, sq ft	0.256
Wing-body combination	
Semispan, with zero gap, in.	8.33
Ratio of body diameter to span with zero gap	0.216

TESTS AND PROCEDURE

The tests were conducted at a Mach number of 1.4 and at a Reynolds number of 2.0×10^6 per foot. Normal-force and pitching-moment data for the body, and normal-force and center-of-pressure data for the wing panels were obtained in the case of zero wing-deflection over an angle-of-attack range of -4° to 16° for each of the nominal gap widths of 0.002, 0.010, 0.050, 0.100, 0.200, 0.400, 0.600, 0.800, 1.00, 2.00, 4.00, and 6.00 inches. Similar data with the body at zero angle of attack were obtained over a range of wing-deflection angles from -2° to 16° at all the same gap-width settings as above except the first. Angles of attack of the wing-body combination included nominal values of $\pm 4^\circ$, $\pm 2^\circ$, $\pm 1^\circ$, 6°, 8°, 12°, and 16°. Since angles of wing deflection could not be varied continuously but had to be set with the tunnel not operating, time limitations restricted these angle settings of $\pm 2^\circ$, 4°, 8°, and 16°. In addition to the data obtained as above by means of the strain-gage equipment, pressure measurements as read on the multiple-tube manometer were recorded photographically at angles of attack of $\pm 2^\circ$, 4°, 8°, and 12° ($\delta = 0$) and at angles of wing deflection of $\pm 2^\circ$, 4°, 8°, and 16° ($\alpha = 0$). A repeat run was made through the angle-of-attack range at the gap-width setting of 0.200 inch to check the repeatability of the data.

The procedure adopted in setting the gap between wing panels and body was to use standard feeler gages for gap widths less than 0.200 inch with the tunnel inoperative, but to employ the motor and calibrated counter to obtain the larger gap widths with the tunnel in operation.

DATA

Reduction

The strain-gage balance on which the body was mounted was calibrated by applying known forces and moments. Body normal force and pitching moment were reduced to coefficient form using the combined area of the two

wing panels as the reference area and the maximum chord of the wing panels as the reference length. The pitching moments were calculated about the hinge line of the wing.

In the case of the strain gages on the wing beams, loads were applied on the wing panels and along the beams at a number of selected stations in order to locate the centers of action of the strain gages on the beams. Calibrations of the moments at two lengthwise stations of each of the cantilevered wing beams were then made by applying known loads at various measured distances from the strain-gage centers. Test data obtained on the wing panels were reduced to normal force and location of resultant normal force as follows:

The sketch below shows the essential features of a wing panel and its supporting beam in the general case of angle of attack and of wing deflection.

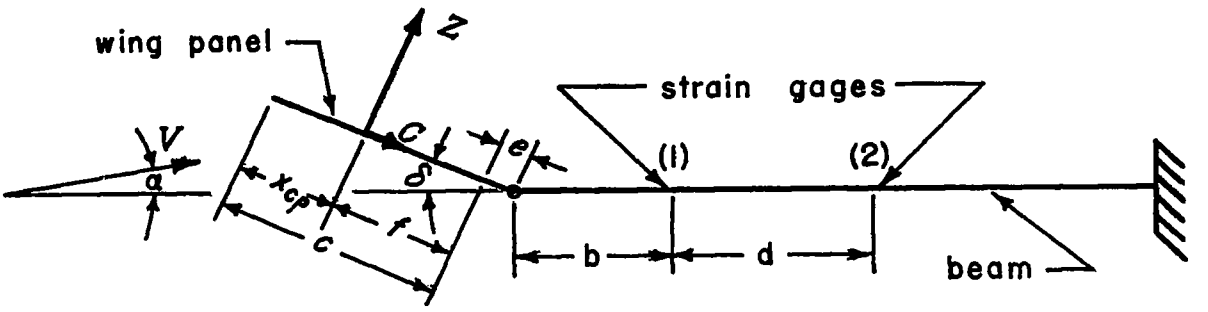

where

Z normal force on wing panel

C chord force of wing panel

c chord of wing panel

b 4.74 in.

d 7.72 in.

e 0.55 in.

The moments about points (1) and (2) in the sketch are, respectively,

$$M_1 = Z(f + e + b \cos \delta) - Cb \sin \delta \tag{1}$$

$$M_2 = Z[f + e + (d + b)\cos \delta] - C(b + d)\sin \delta \tag{2}$$

from which

$$M_2 - M_1 = Zd \cos \delta - Cd \sin \delta \tag{3}$$

and

$$Z = \frac{M_2 - M_1}{d \cos \delta} + C \tan \delta \tag{4}$$

Also, from equations (1) and (2)

$$x_{cp} = c - f = c + e - \frac{M_1 + Cb \sin \delta}{M_2 - M_1 + Cd \sin \delta} d \cos \delta + b \cos \delta \tag{5}$$

In the case of the undeflected wing ($\delta = 0$), equations (4) and (5) become

$$Z_{(\delta=0)} = \frac{M_2 - M_1}{d} \tag{6}$$

and

$$(x_{cp})_{(\delta=0)} = c + e + b - \frac{d}{(M_2/M_1) - 1} \tag{7}$$

so that the chord force C need not be taken into account. Inasmuch as M_1 and M_2 are computed from the calibration which involved only normal loads, and since the product of the chord force C and the sine or tangent of the angle of wing deflection in the present test is very small compared to the normal force, the equations used to compute Z and x_{cp} for the deflected wing panels were obtained from equations (4) and (5) by neglecting the effect of the unknown chord force. Thus, for the wing deflection case

$$Z = \frac{M_2 - M_1}{d \cos \delta} \tag{8}$$

$$x_{cp} = c + e - \left[\frac{d}{(M_2/M_1) - 1} - b\right]\cos \delta \tag{9}$$

Normal force and hinge moments on each of the two wing panels were reduced to coefficient form in the same manner as for the body and were averaged to give values for the wing. Likewise, the positions of the center of pressure were nondimensionalized in terms of the root chord of the wing panels and were averaged.

Corrections to angle of attack of the body were made from the results of a deflection calibration of the model sting. A correction was also applied to take into account the necessary but small clearances between the body and the strain-gage balance. This latter correction had a magnitude of 0.15°.

Calibration was also made to determine the effect of magnitude and location of normal loads of the wing panels on the increase of wing incidence. At the widest gap width (6 in.), the increase in the incidence of the wing was somewhat greater than that at narrow gap widths; however, the rate of increase of angular deflection with normal loads obtained for small gaps was used to compute values of wing deflection at all gap settings. The corrections applied to the nominal values of wing-deflection angles depended upon both magnitude of normal force and the position of the center of pressure of the wing, and were as large as 0.89° at the largest angle of attack with a gap width of 0.010 inch.

In order to obtain the variation of normal force with angle of attack under the condition of zero wing deflection, the included effects of the load-induced wing deflections were estimated from the variation of normal force with δ and subtracted from the normal forces obtained in the angle-of-attack case. No account was taken of the slight displacement of the wing out of the diametral plane of the body due to the bending of the supporting structure of the wing panels.

Some stream curvature at supersonic speeds has been seen to exist in the yaw plane of the model (ref. 8). However, results presented in reference 9 indicate that the effects of this curvature on the measured characteristics of the present model should be small.

No attempt was made to measure the magnitude of external forces on the wing beams due to the downwash from the model. However, although complete shielding of the beams seemed impractical, cover plates were installed across the strain gages of the beams in such a manner that the major portion of any external loads would be carried by the beam aft of the most rearward strain gage. In addition, the width of the beams was kept as small as was compatible with structural strength requirements,

so that any aerodynamic effects on the beams would be minimized. In comparison with the moments engendered by the wing panels at the two strain-gage positions on the beams, the corresponding moments due to any external forces acting on the beams themselves are judged to be so small as not to affect the results of the tests within the limits of measuring accuracy. The repeatability of the data indicated that normal-force coefficients of the wing panels could be measured to within ±0.01 and the angle of attack and wing deflection could be set to within ±0.10°.

Normal forces on that portion of the body included between stations opposite the apex and trailing edge of the wing were obtained by double graphical integration of the plotted pressure data. Although the number of pressure orifices on the body was insufficient for a high degree of accuracy in determining absolute values of normal force, greater faith is placed in the accuracy of the ratios of normal forces obtained with gaps present to those with zero gap.

RESULTS AND DISCUSSION

Variations of normal force with angle of attack for the wing, complete body, and body exclusive of nose and afterbody in the case of zero wing deflection are given for a number of gap widths in figure 3. Figure 4 presents corresponding results for zero angle of attack and variable wing deflection. From these two figures, and from similar plots for other gap widths not shown, the variations with gap width of the ratio of lift to lift with zero gap shown in figure 5 were obtained. The value for the lift with zero gap in the angle-of-attack case was taken as the value obtained at the smallest gap width tested, 0.002 inch. In the case of wing deflection, the smallest gap width for which data were obtained was 0.010 inch, so a large-scale plot of C_Z versus gap width in inches was used to extrapolate down to a 0.002-inch gap for the value of C_Z with zero gap. This procedure is believed to have given conservatively low values for zero-gap lifts in each case.

Figure 6 shows the effect upon the lift of the wing-body combination of relatively small gaps and points out more clearly than figure 5 the discrepancies between theoretical and experimental results.

The effect of gap upon the effectiveness of the all-movable wing as a control surface is shown in figure 7. The experimental effectiveness parameter, $-\frac{d\alpha}{d\delta}$ defined by

$$-\frac{d\alpha}{d\delta} = \frac{(\partial C_Z/\partial \delta)_{C_Z=0}}{(\partial C_Z/\partial \alpha)_{C_Z=0}}$$

was obtained by measuring the initial slopes of the curves presented in figures 3 and 4.

Figures 8, 9, and 10 show the effect of gap upon the moment characteristics of the wing and body for the case of zero angle of attack and variable wing deflection.

Effect of Gap Upon Lift Characteristics

Wing.- One particularly noticeable effect of gap upon the lift characteristics of the wing is apparent in figures 3(a) and 4(a), namely the introduction of nonlinearity into the curves of normal force versus α and δ. The reasons for the nonlinearity for small gaps and large gaps are believed to be different. At very small gap widths (less than 0.2 inch), the gap produces a noticeable loss in normal force for small α or δ but none or little at larger angles. That the percentage losses in lift at angles near zero are not as large as predicted by theory (fig. 5(a)) is attributed chiefly to viscous effects; at larger angles and with very small gaps, the percentage loss in lift is essentially zero, presumably because the flow in the gap is choked. In the case of the wider gaps, the nonlinearity of the normal-force curves may be the phenomenon found for low-aspect-ratio wings, since each wing panel tends to act as an independent low-aspect-ratio wing. Other factors involved in the observed gap effects might well include the effects of the boundary layer surrounding the body and of the shock waves emanating from the apexes of the wing panels.

Figure 5(a) shows that the slender-body theory of reference 3 agrees reasonably well with the small-angle experimental results for the wing of the wing-body combination in the wider gap range, considering that the test model was only moderately slender in the terminology of the theory. (The experimental lift ratios shown for values of α and δ between 0° and 1° were obtained from the initial slopes of the curves of figures 3 and 4.) Even closer agreement between theory and experiment is obtained in the case of wing deflection ($\alpha = 0$) by applying the methods of reference 4 in which the body is assumed to carry no lift but to act as a perfect reflecting plane, and in which the lift ratio for the "effectively infinite" gap width (equal to 0.680 wing semispan for the present test model) was calculated by means of linearized supersonic theory.

Body.- As in the case of the wing, one effect of a gap upon the lifting characteristics of the body is the comparatively large decrease in normal force for angles of attack or of wing deflection near zero and the smaller decreases at larger angles (figs. 3(b), 3(c), 4(b), and 4(c)). The nonlinear variation of body normal force with angle of attack or of wing deflection is probably due in large part to the same phenomena suggested above in connection with the effects of gaps upon the lift of the

wing. In addition, there might be mentioned the viscous cross force on the body at the wider gaps, and the effects of the vertically displaced pressure fields of the deflected wing panels.

Figure 5(c) shows that for angles of attack or of wing deflection near zero, slender-body theory predicts quite well the percent losses in lift on that portion of the body exclusive of nose and afterbody, except for the two or three smaller gap widths tested. It is interesting to note the effect of the afterbody (not included in the theoretical results of ref. 3) on the lift ratios. In the case of wing deflection, where the nose carries no lift ($\alpha = 0$), the experimental data indicate that at angles near zero the portion of the total body lift carried by the afterbody increases from 12 percent at zero gap (extrapolated) to 23 percent at a gap of 0.012 semispan, but is zero for gaps of 0.048 semispan and larger. This variation of afterbody lift is reflected in figure 5(b) which shows that the percent losses in lift are somewhat smaller for the above narrow gaps and slightly larger for the wider gaps than those given in figure 5(c), $\alpha = 0$. At larger angles of wing deflection, lift is apparently recovered through the upwash induced by the wing on the afterbody at all gap widths, and the percent losses due to gap effects are thus reduced from those which would obtain if there were no afterbody.

In the case of angle of attack ($\delta = 0$), comparison of figure 5(b) with 5(c) gives the combined effects of nose and afterbody lift in modifying the percent losses in lift due to gap. The theory presented, which does not include the lift of the afterbody, predicts smaller losses in lift, percentagewise, when the lift of the body nose is added to the body lift induced by the wing because at supersonic speeds the lift of the nose is unaffected by the gap. At angles of attack near zero, however, the experimental results show just the opposite trend for gap widths less than 10 percent of the semispan when the lifts of both nose and afterbody are added to the induced body lift. Evidently in the angle-of-attack case the losses in lift of the afterbody at small gaps and small angles more than offset the effect of the nose lift. With increasing angle of attack, the data show that an increasingly larger portion of the body lift is carried by the nose so that the percent losses shown in figure 5(b) for the body inclusive of nose and afterbody at the two larger angles are smaller than those given in figure 5(c), $\delta = 0$.

Wing-body combination.- The results obtained individually for the wing and body are combined to give the effects of gap upon the lift of the wing-body combination in figures 5(d), 6(a), and 6(b).

Agreement between theoretical and experimental results at angles near zero is fortuitously closer in the angle-of-attack case when the lift of the nose and afterbody is included (fig. 6(a), $\delta = 0$) than when such lift is not included (fig. 6(b), $\delta = 0$). This closer agreement in the first instance is due to the fact that although the theory overestimates the percent losses in the lift of the wing and of the body exclusive

of the nose and afterbody, it underestimates such losses in the case of the body when the lift of nose and afterbody is included, as explained in the preceding section. Similarly, the theory is closer to measured values in the angle-of-attack case ($\delta = 0$) than in the case of wing deflection ($\alpha = 0$) since the nose carries no lift in the latter case and the above compensating effects are absent. (See fig. 5(d).)

Results shown in figure 5(d) indicate that only for angles of attack or of wing deflection near zero and for gaps wider than 5 percent of the wing semispan does slender-body theory predict satisfactorily the percent losses in lift due to gap effects. The percent losses in lift with narrower gaps, although significant at small angles ($\alpha,\delta < 5^{\circ}$), are only fractions of those predicted in the theory. In the range of small gap widths, the discrepancies between theory and experiment are more easily seen in figure 6(a), where the scale of gap-width parameter has been increased fivefold. For example, figure 6(a) shows that whereas theory predicts a 25-percent loss in lift due to a gap width of 0.1 percent of the wing semispan, the corresponding experimental loss is only 7 percent for small angles of attack and is zero for angles of attack greater than 5°. Similar comparisons can be made in the case of wing deflection.

For all gap widths tested, figure 5(d) shows that percent losses in lift decrease with increasing angle of attack ($\delta = 0$) or of wing deflection ($\alpha = 0$). This effect is more noticeable for angles of attack than for angles of wing deflection, and is relatively larger for narrow than for wide gaps. As a consequence, although percent losses in lift due to gap effects are more severe in the case of $\delta = 0$ than in that of $\alpha = 0$ for small angles as predicted by theory, the reverse is true for angles as large as 5° or more, except for the wider gaps.

It is interesting to note in figure 6(a), $\alpha = 0$, that the approximation for the gap effects upon lift made by Mirels in reference 2 is remarkably close to the analytic result of reference 3.

Effect of Gap Upon Effectiveness of All-Movable Wing as a Control Surface

It is often of interest to compare the lift obtained by a given deflection of a wing control surface with that due to an equal angle of attack. For the present test model, the entire wing is the control surface. The usual parameter employed to express the effectiveness of a control surface is

$$-\frac{d\alpha}{d\delta} = \left(\frac{\partial C_L/\partial\delta}{\partial C_L/\partial\alpha}\right)_{C_L = \text{const.}}$$

Inasmuch as the variation of normal force of wing or body is not linear with angle of attack or of wing deflection beyond 1° or 2° with a gap present, the results shown in figure 7 are restricted to angles near zero (or to very small lift coefficients).

Figure 7(a) shows that the theory agrees in a qualitative manner with the present experiment, but that the quantitative agreement is relatively poor for gap widths smaller than 20 percent of the wing semispan.

Comparison of figure 7(a) with figure 7(b) again demonstrates the fortuitous improvement in agreement of theoretical with experimental results when the lifts of the nose and afterbody are taken into account.

Effect of Gap Upon Hinge Moment Due to Wing Deflection

Unfortunately, the precision with which hinge-moment coefficients could be calculated (±0.004) from the experimentally obtained data is of much the same order of magnitude as the values of the coefficients themselves in the range of wing deflection angles from 0° to 4°. Consequently, no very high trust can be placed in the peculiar variation of the hinge moment with normal force observed in figure 8 at the smaller values of the latter. Only at the higher values of normal force can a consistent trend of variation of hinge moment with gap width be observed; namely, a decrease in hinge moment for a given normal force with increasing gap width for a range of gap width extending to approximately 5 percent of the wing semispan, followed by a monotonic increase with further increase in gap width. The corresponding travel of the center of pressure is shown in figure 9. (No curves for small angles of wing deflection are given due to unreliability of the data at low values of normal force.) The slender-body theoretical results of reference 4 are also given in figure 9 for comparison. As can be seen, the experimental effects of gap upon the chordwise location of the center of pressure of the deflected wing bear a qualitative resemblance to those given by theory. However, the range of travel of the center of pressure due to gap effects is more extreme and farther forward on the wing than indicated by slender-body theory.

Effect of Gap Upon Pitching Moment of Body Due to Wing Deflection

In general, figure 10 shows that for a given normal force induced on the body by the deflected wing, the pitching moment of the body about the hinge line is negative and first increases in absolute value with increasing gap width to a maximum value at small gap width, and thereafter decreases with wider gaps. The travel of the center of pressure on the

body is thus somewhat similar to that noted for the wing in the preceding section, although the resultant of the body normal forces is aft of the hinge line rather than forward as on the wing (due, no doubt, to the effect of the afterbody).

CONCLUSIONS

From the results of the experimental investigation of the effects of gap upon the lift and pitching moment of a moderately slender wing-body combination at a Mach number of 1.4, the following conclusions are indicated:

1. Introduction of a gap between wing and body resulted in a nonlinear variation of lift with angle of attack and of wing deflection. The large percent losses in lift due to gap predicted by theory were sensibly realized only for angles of attack or of wing deflection near zero and for gap widths larger than 5 percent of the wing semispan. For gap widths less than 1 percent of the wing semispan, significant losses in lift occurred only at angles of attack or of wing deflection near zero.

2. At all gap widths tested, the percent losses in lift decreased with increasing angle of attack or of wing deflection, more so in the case of angle of attack than in the case of wing deflection.

3. As predicted by theory, the percent losses in lift due to gap were larger in the angle-of-attack case than in the case of wing deflection for small angles. At larger angles, the reverse was found to be true for small gap widths.

4. In general, the center of pressure of wing and body in the case of wing deflection ($\alpha = 0$) moved rearward with increasing small gap widths but reversed this trend with yet wider gaps.

5. The length of the afterbody may be of significance in determining the percent losses in lift due to gap, particularly in the case of zero wing deflection.

Ames Aeronautical Laboratory
National Advisory Committee for Aeronautics
Moffett Field, Calif., Apr. 8, 1955

REFERENCES

1. von Kármán, Th., and Burgers, J. M.: General Aerodynamic Theory - Perfect Fluids. Vol. II of Aerodynamic Theory, div. E, W. F. Durand, ed., Julius Springer (Berlin), 1934.

2. Mirels, H.: Gap Effect on Slender Wing-Body Interference. Readers' Forum, Jour. Aero. Sci., vol. 20, no. 8, Aug. 1953, pp. 574-575.

3. Dugan, Duane W., and Hikido, Katsumi: Theoretical Investigation of the Effects Upon Lift of a Gap Between Wing and Body of a Slender Wing-Body Combination. NACA TN 3224, 1954.

4. Bleviss, Z. O., and Struble, R. A.: Some Effects of Streamwise Gaps on the Aerodynamic Characteristics of Low-Aspect-Ratio Lifting Surfaces at Supersonic Speeds. Douglas Rep. SM-14627, Apr. 1953.

5. Munk, M., and Cario, G.: Flugel mit Spalt in Fahrtrichtung. vol. 1, Technische Berichte der Flugzeugmeisterei, 1917, p. 219.

6. Drake, William C.: Lift, Drag, and Hinge Moments at Supersonic Speeds of an All-Movable Triangular Wing and Body Combination. NACA RM A53F22, 1953.

7. Bailey, H. E., and Phinney, Ralph E.: Final Report. Wing-Body Interference, Part III. Experimental Investigation of Body Simulator Plate. Eng. Res. Inst., Univ. of Mich., Contract AF 33 (038) - 19747, Feb. 1954.

8. Frick, Charles W., and Olson, Robert N.: Flow Studies in the Asymmetric Adjustable Nozzle of the Ames 6- by 6-Foot Supersonic Wind Tunnel. NACA RM A9E24, 1949.

9. Lessing, Henry C.: Aerodynamic Study of a Wing-Fuselage Combination Employing a Wing Swept Back 63° - Effect of Sideslip on Aerodynamic Characteristics at a Mach Number of 1.4 With the Wing Twisted and Cambered. NACA RM A50F09, 1950.

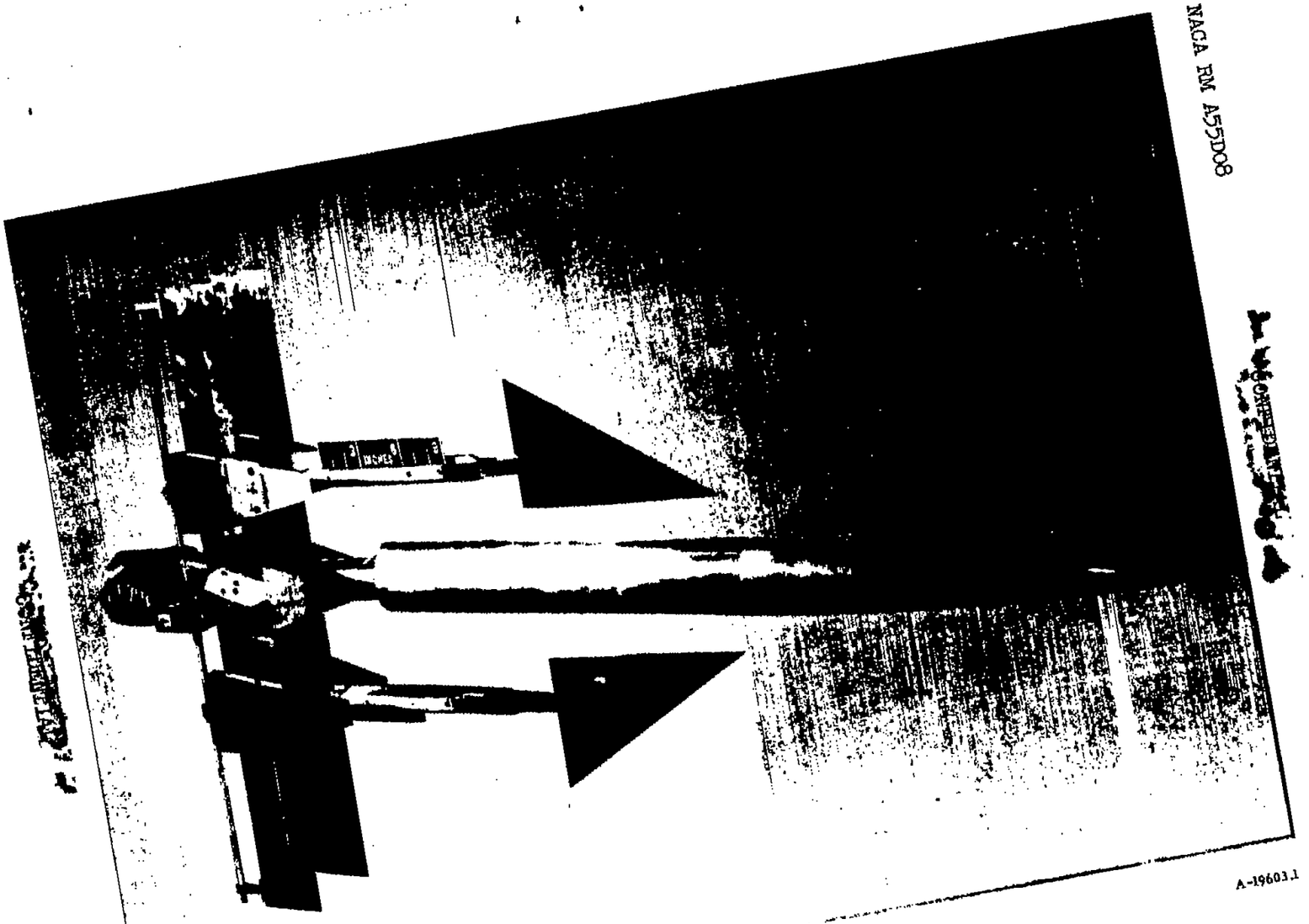

A-19603.1

Figure 1.- Photograph of test model.

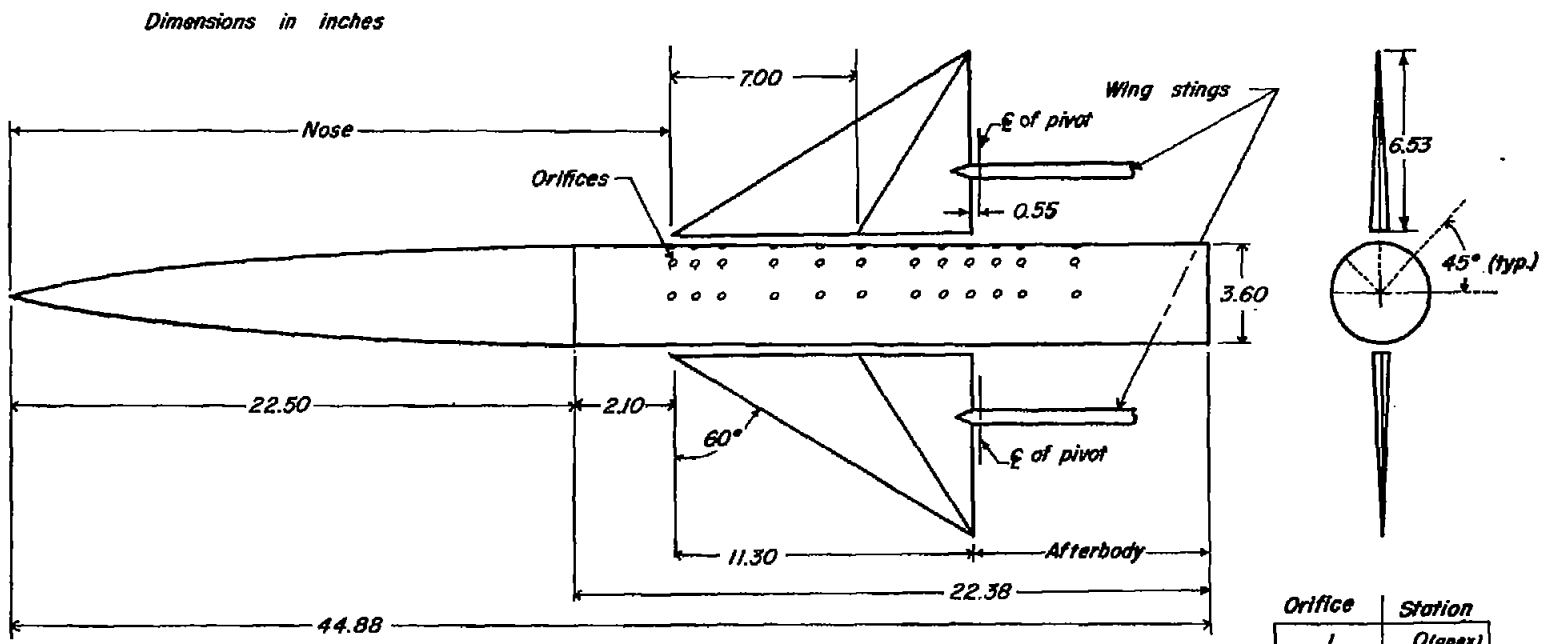

Orifice	Station
1	0(apex)
2	1.00
3	2.00
4	4.00
5	5.65
6	7.30
7	9.30
8	10.30
9	11.30
10	12.30
11	13.30
12	

Figure 2.- Details of test model.

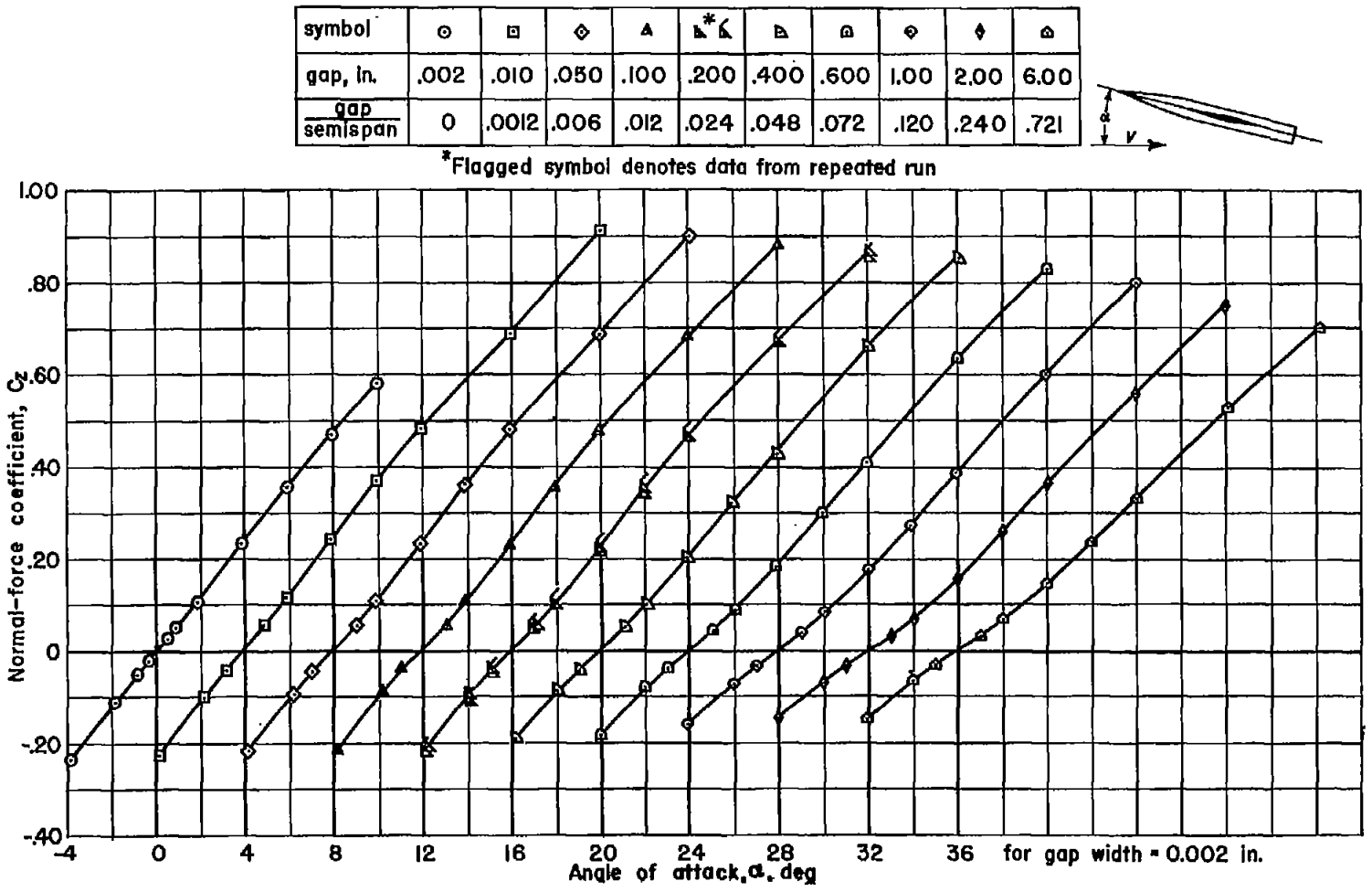

(a) Wing.

Figure 3.- Effect of gap width on variation of normal force with angle of attack; δ = 0.

symbol	⊙	⊡	◇	▲	◣*◣	◺	⌂	◈	◊	⌂
gap, in.	.002	.010	.050	.100	.200	.400	.600	1.00	2.00	6.00
$\frac{\text{gap}}{\text{semispan}}$	0	.0012	.006	.012	.024	.048	.072	.120	.240	.721

*Flagged symbol denotes data from repeated run

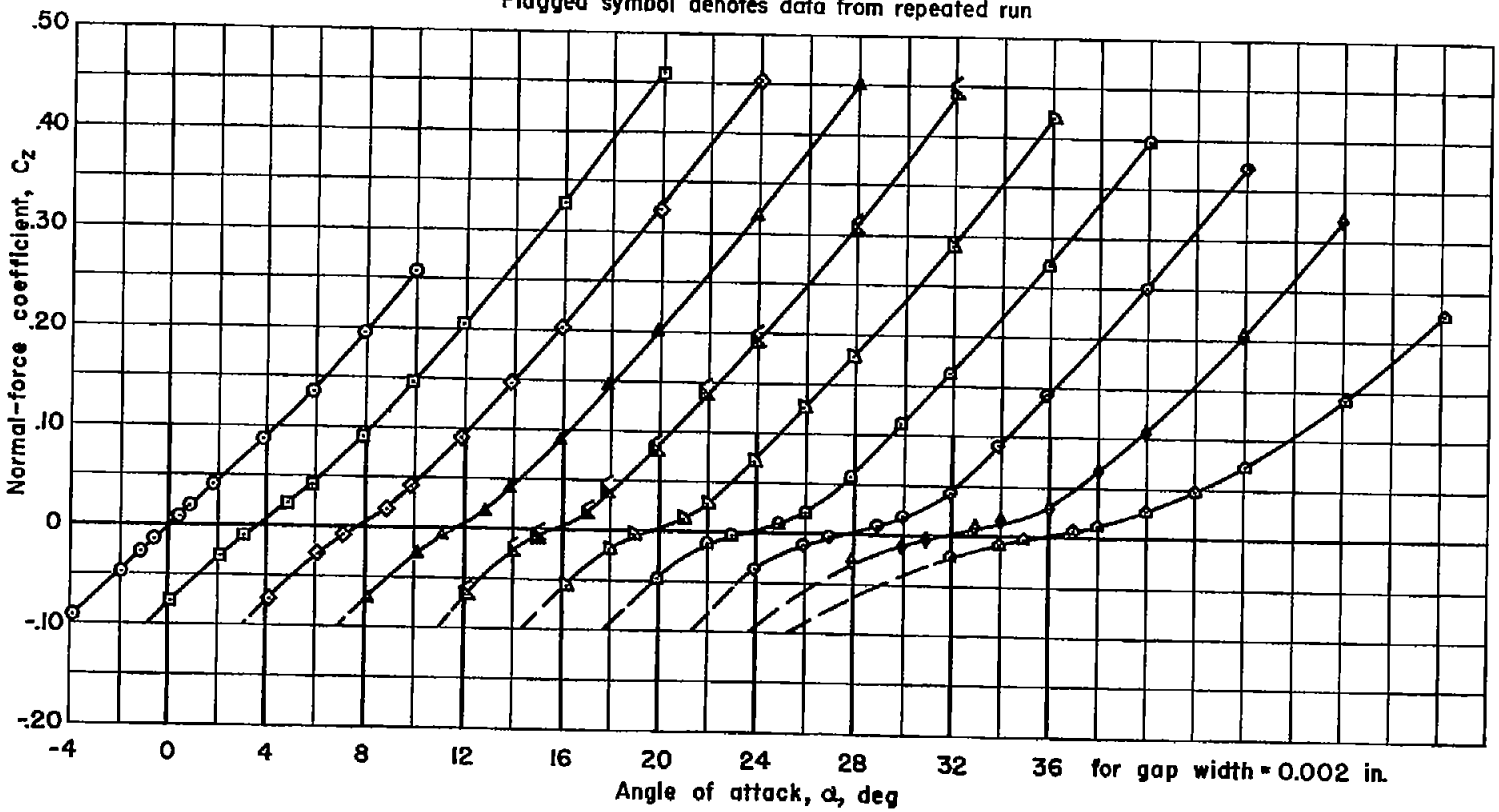

(b) Body, including nose and afterbody.

Figure 3.- Continued.

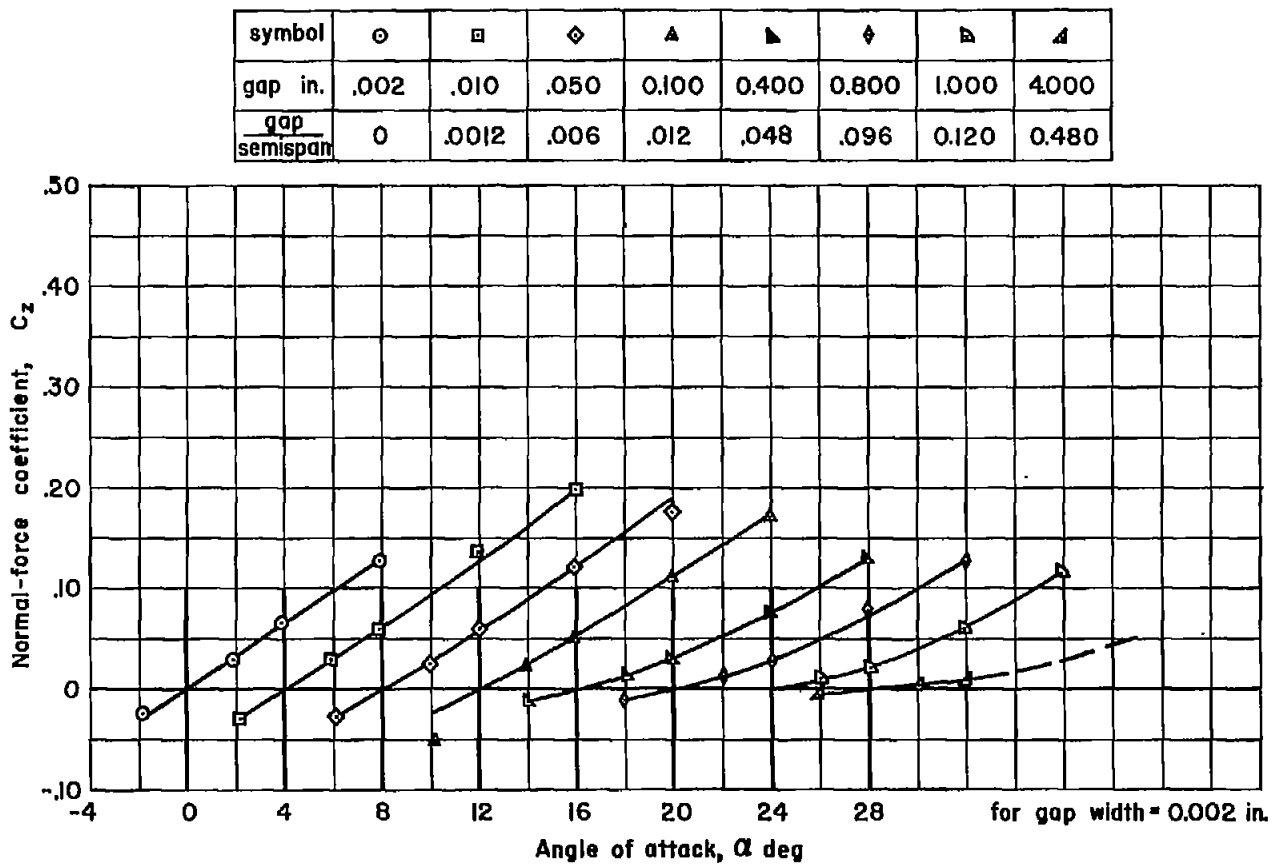

(c) Body, excluding nose and afterbody.

Figure 3.- Concluded.

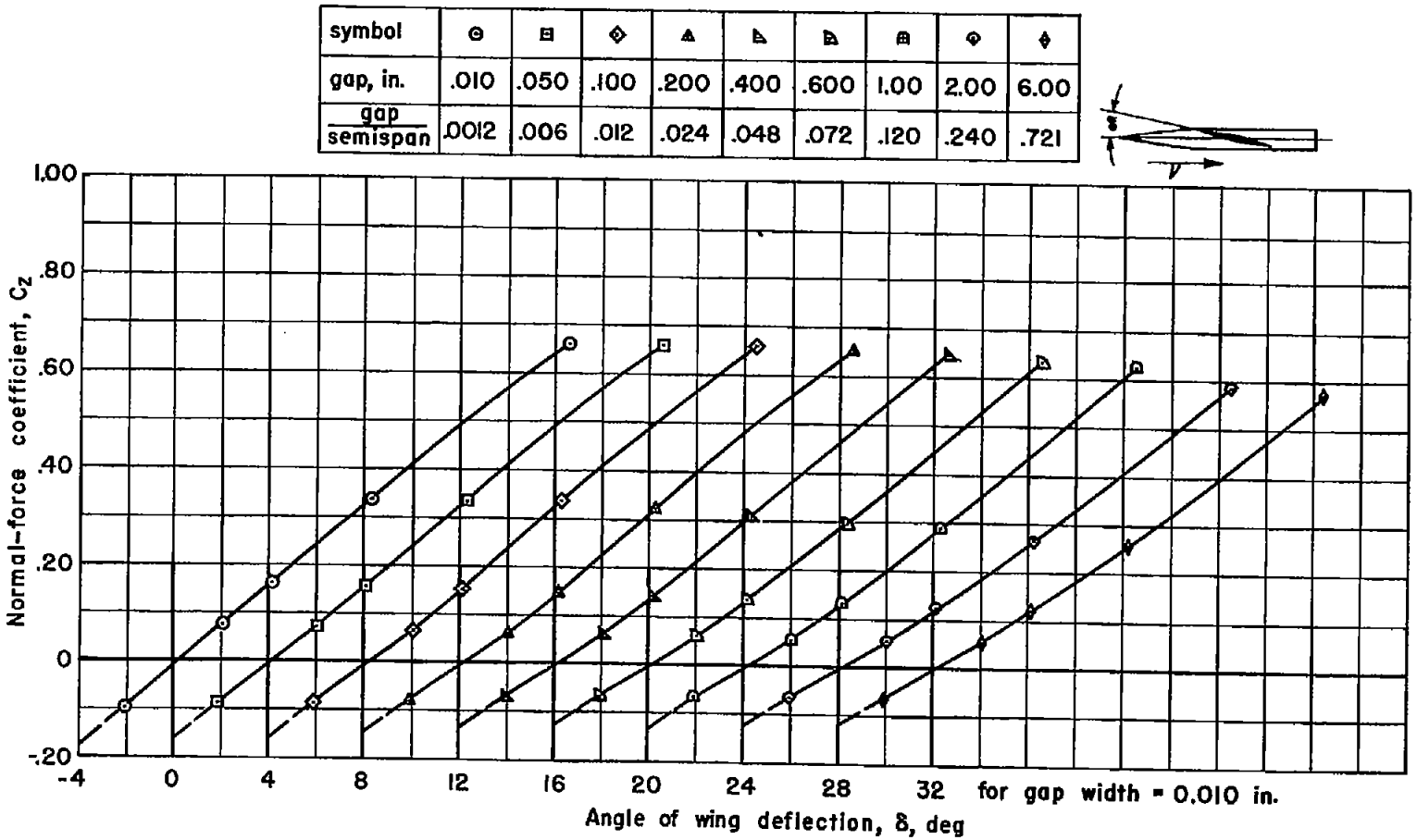

(a) Wing.

Figure 4.- Effect of gap width on variation of normal force with angle of wing deflection; $\alpha = 0$.

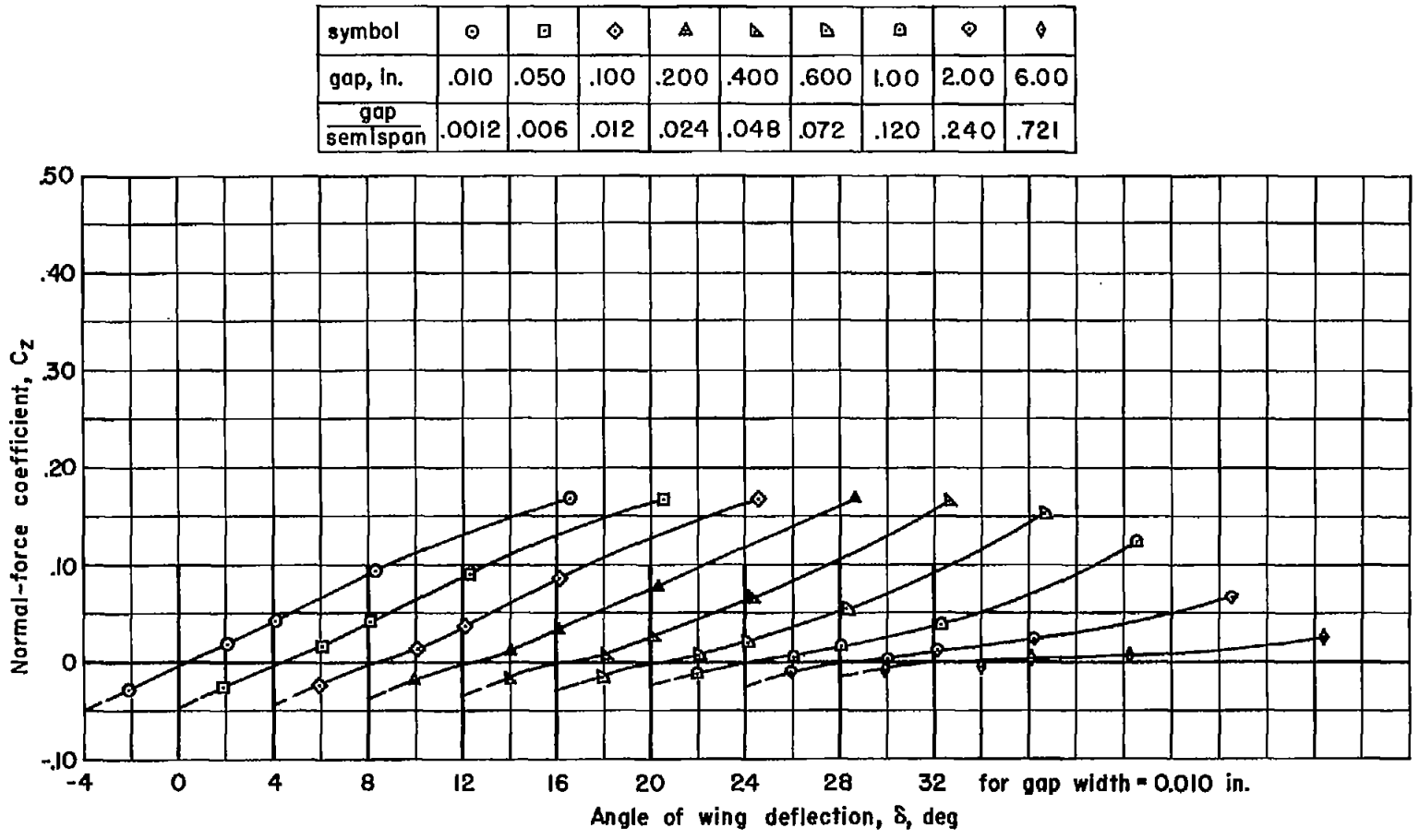

(b) Body, including nose and afterbody.

Figure 4.- Continued.

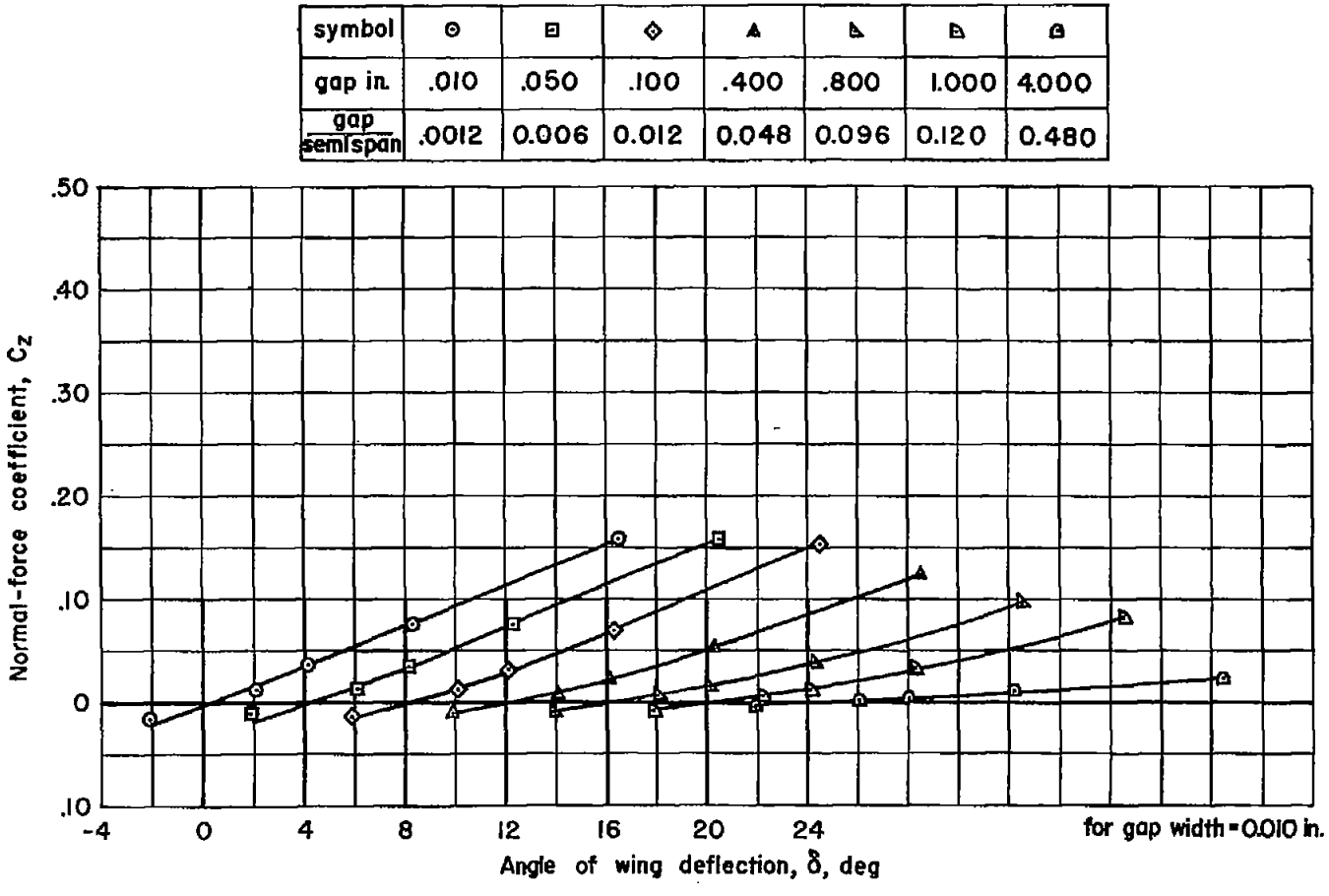

(c) Body, excluding nose and afterbody.

Figure 4.- Concluded.

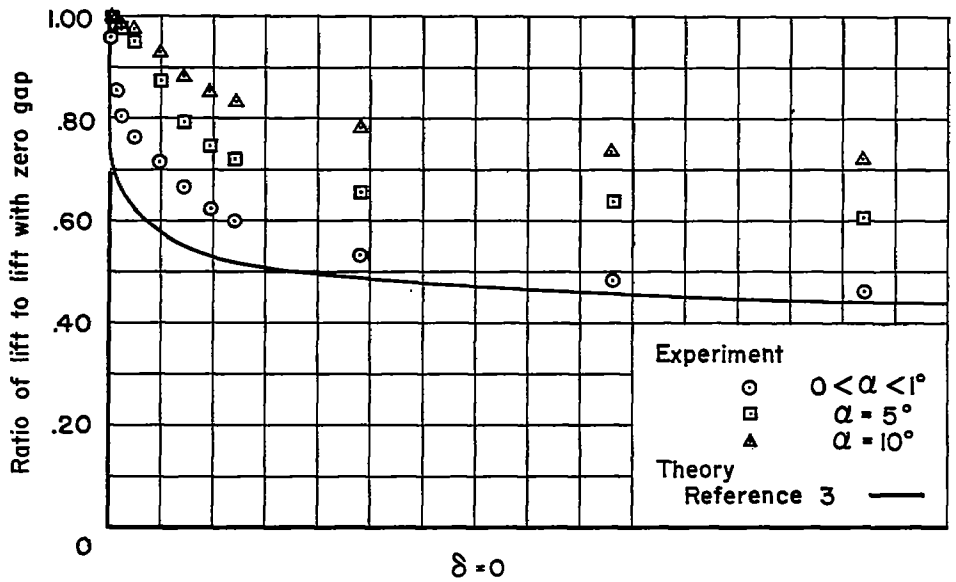

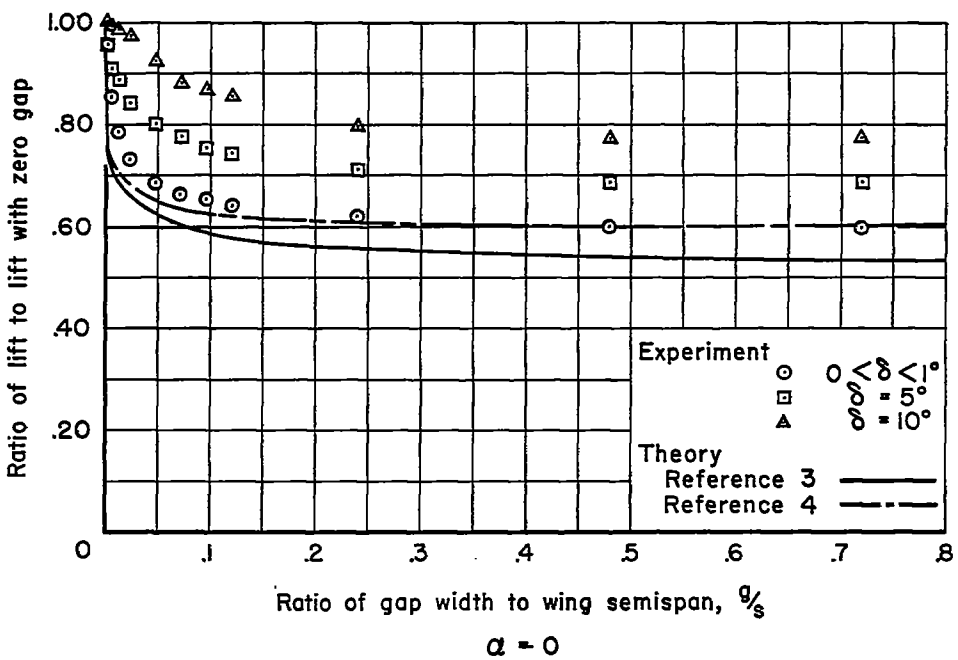

(a) Wing.

Figure 5.- Effect of gap between wing and body upon lift.

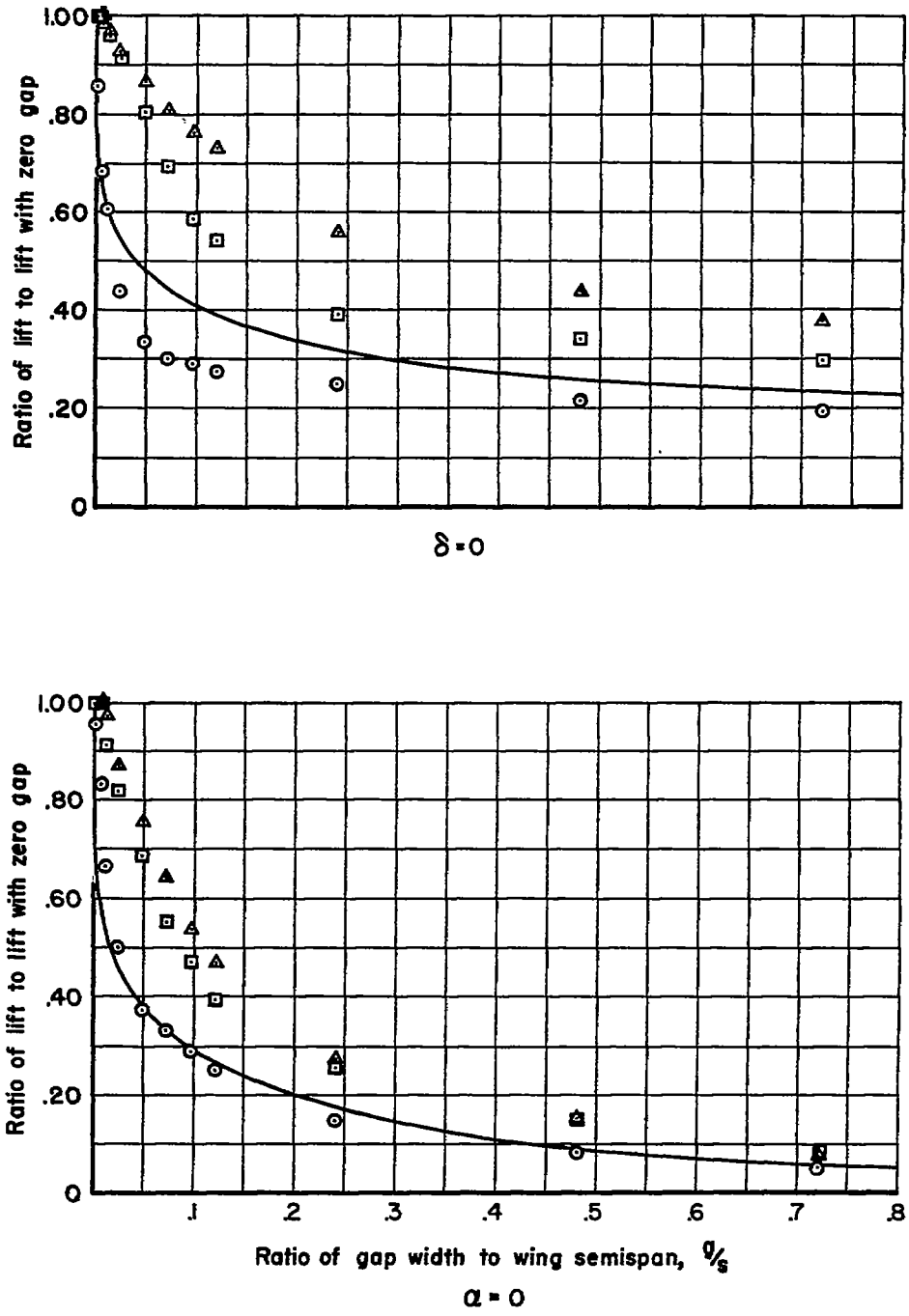

(b) Body (experiment includes nose and afterbody; theory includes nose only).

Figure 5.- Continued.

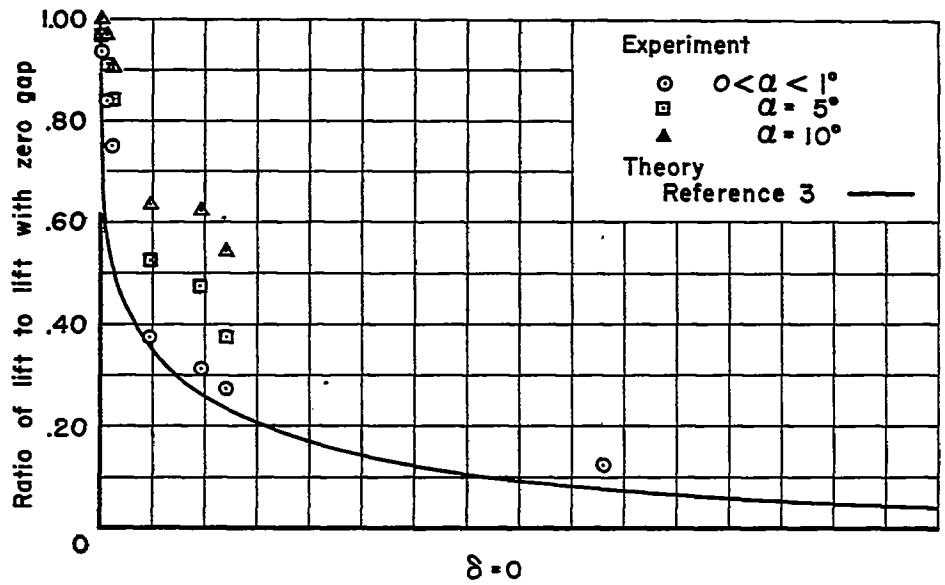

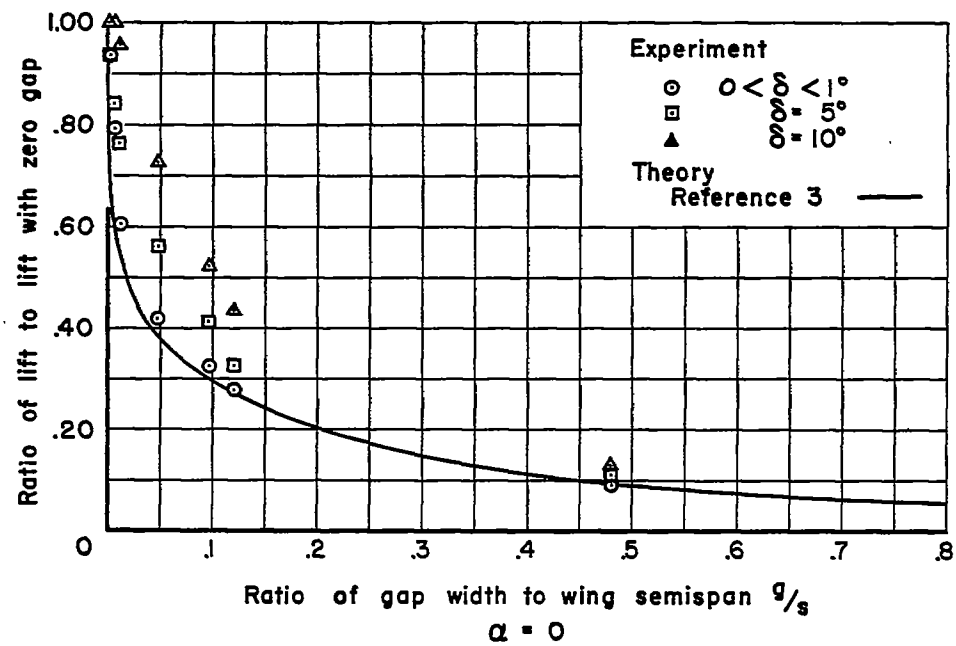

(c) Body, excluding nose and afterbody.

Figure 5.- Continued.

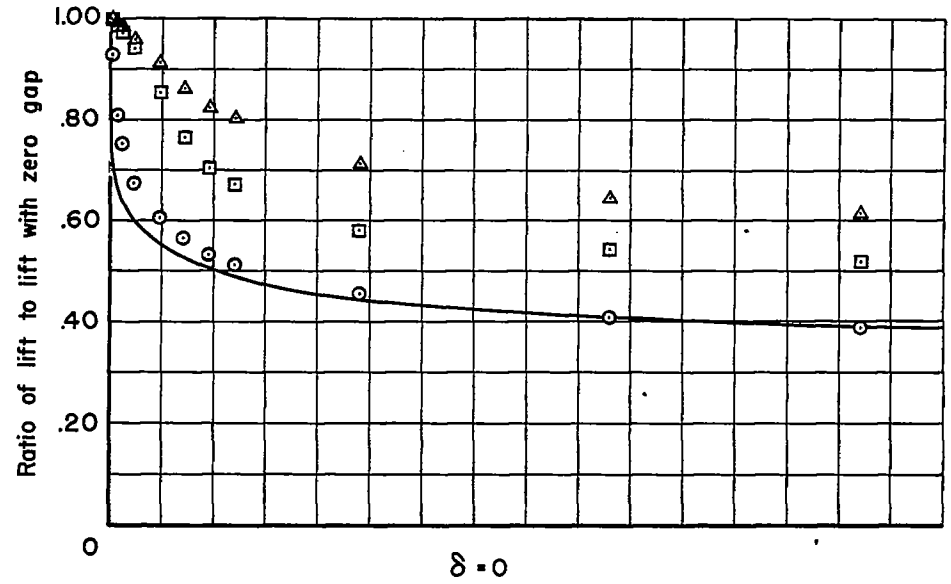

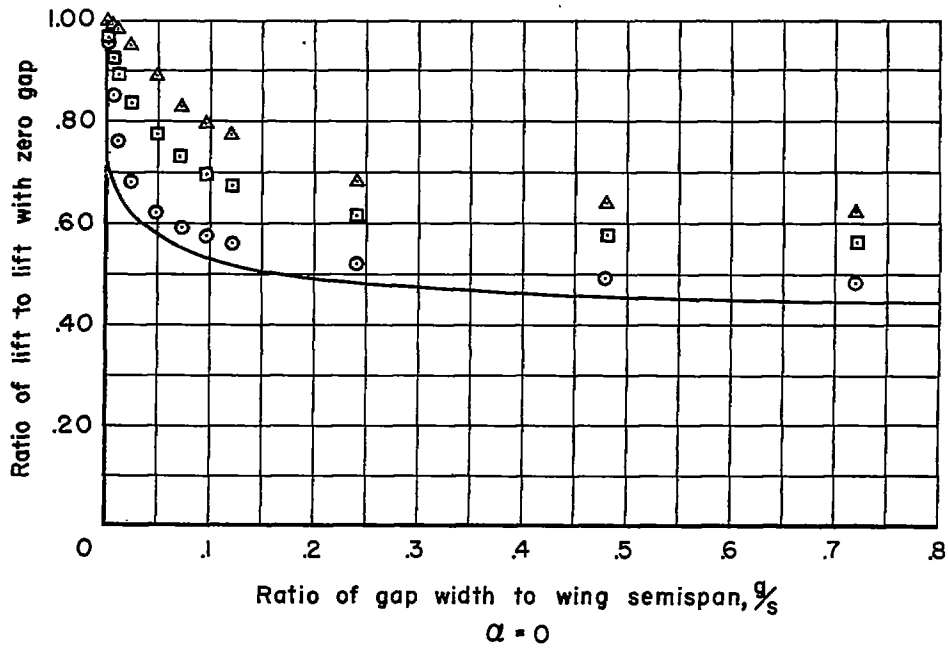

(d) Wing-body combination (experiment includes nose and afterbody; theory includes nose only).

Figure 5.- Concluded.

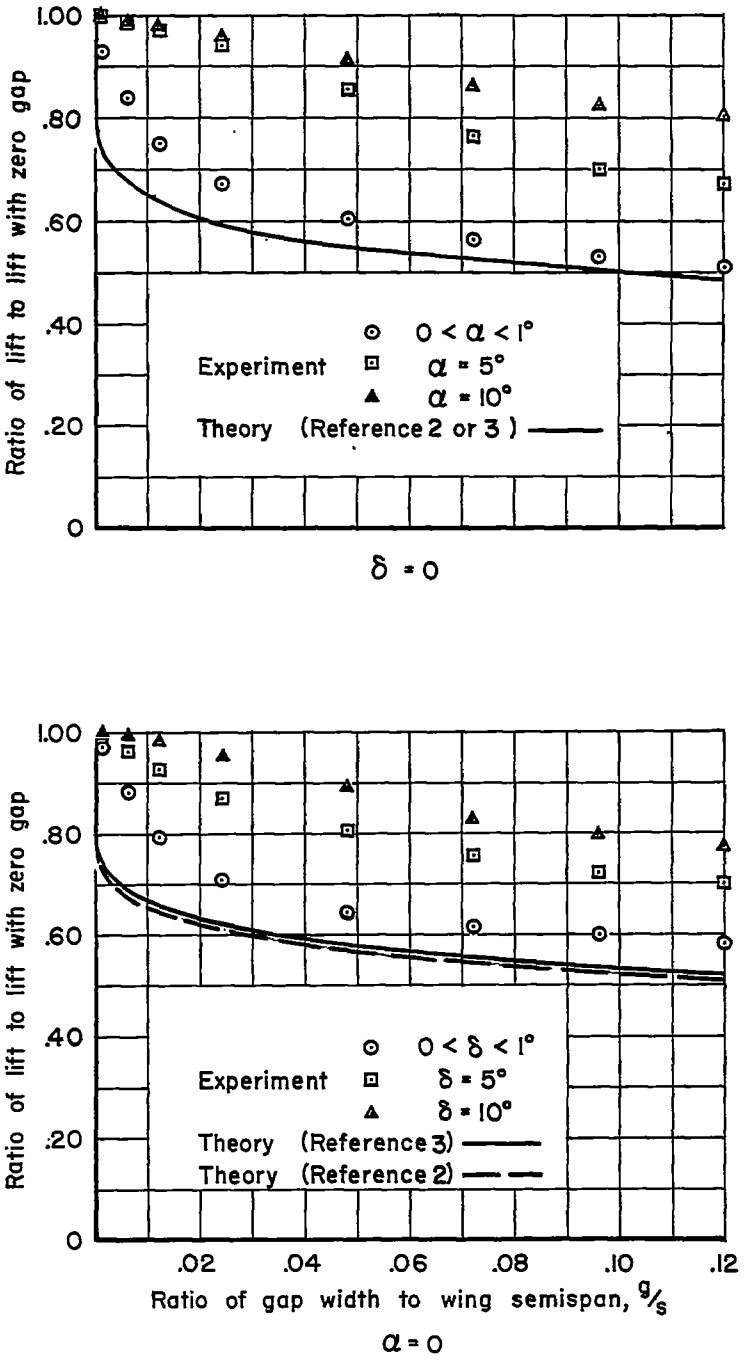

(a) Lift of nose and afterbody included in experiment (no afterbody in theory).

Figure 6.- Effect of gap between wing and body upon lift of wing-body combination for relatively small gaps.

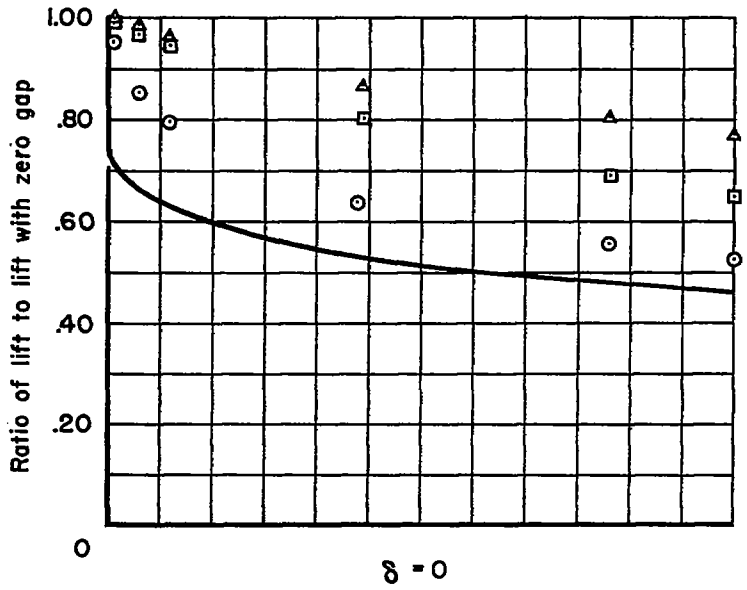

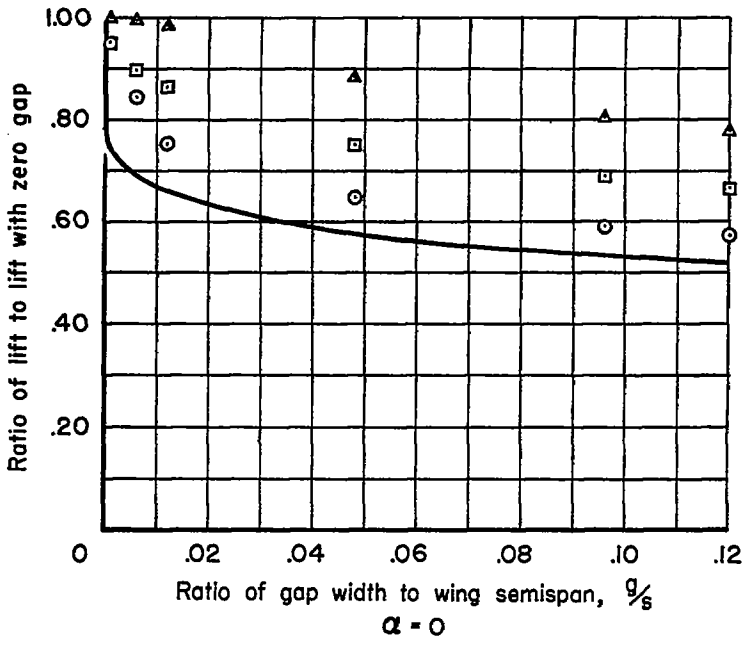

(b) Lift of nose and afterbody excluded.

Figure 6.- Concluded.

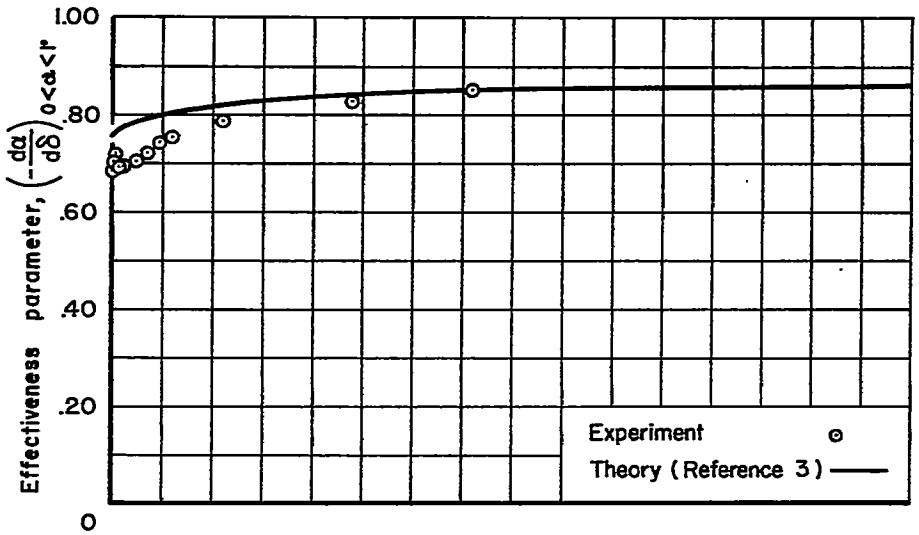

(a) Wing-body combination including lift of nose and afterbody in experiment (no afterbody in theory).

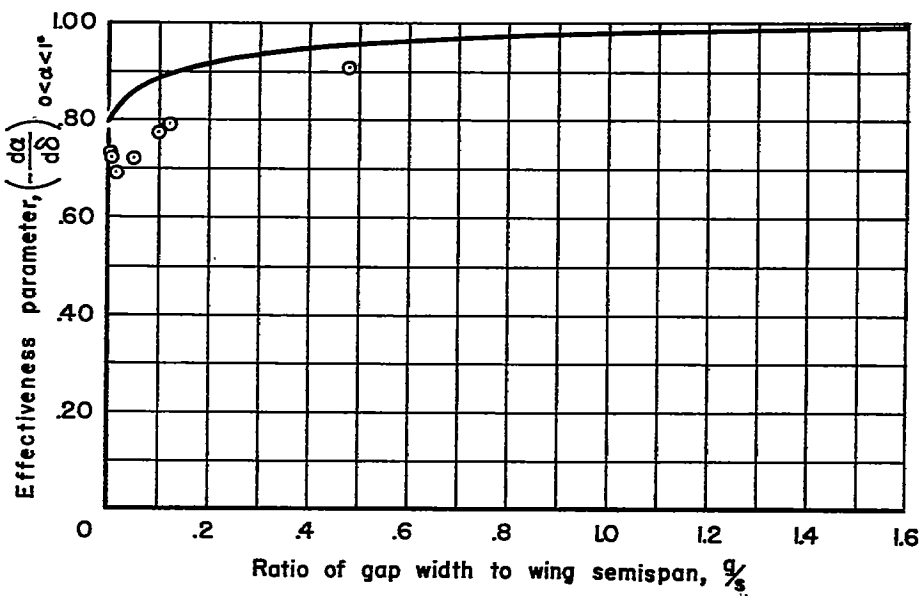

(b) Wing-body combination excluding lift of nose and afterbody.

Figure 7.- Effect of gap upon effectiveness of all-movable wing as a control surface.

symbol	⊙	⊡	◇	▲	◣	◺	⌂	⊙	◆	⌂
gap, in.	.010	.050	.100	.200	.400	.600	1.00	2.00	4.00	6.00
$\frac{\text{gap}}{\text{semispan}}$	.0012	.006	.012	.024	.048	.072	.120	.240	.481	.721

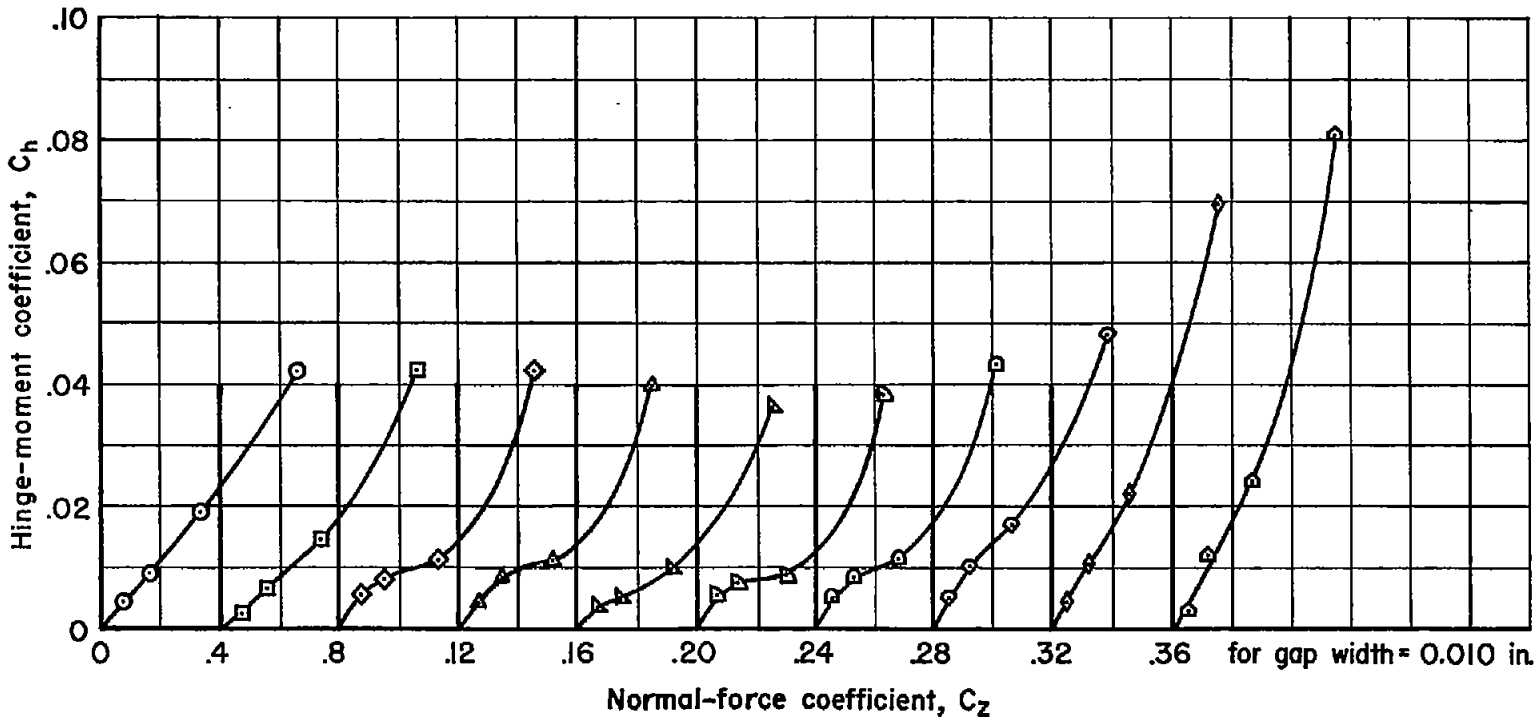

Figure 8.- Effect of gap upon variation of hinge moment of all-movable wing with normal force; $\alpha = 0$.

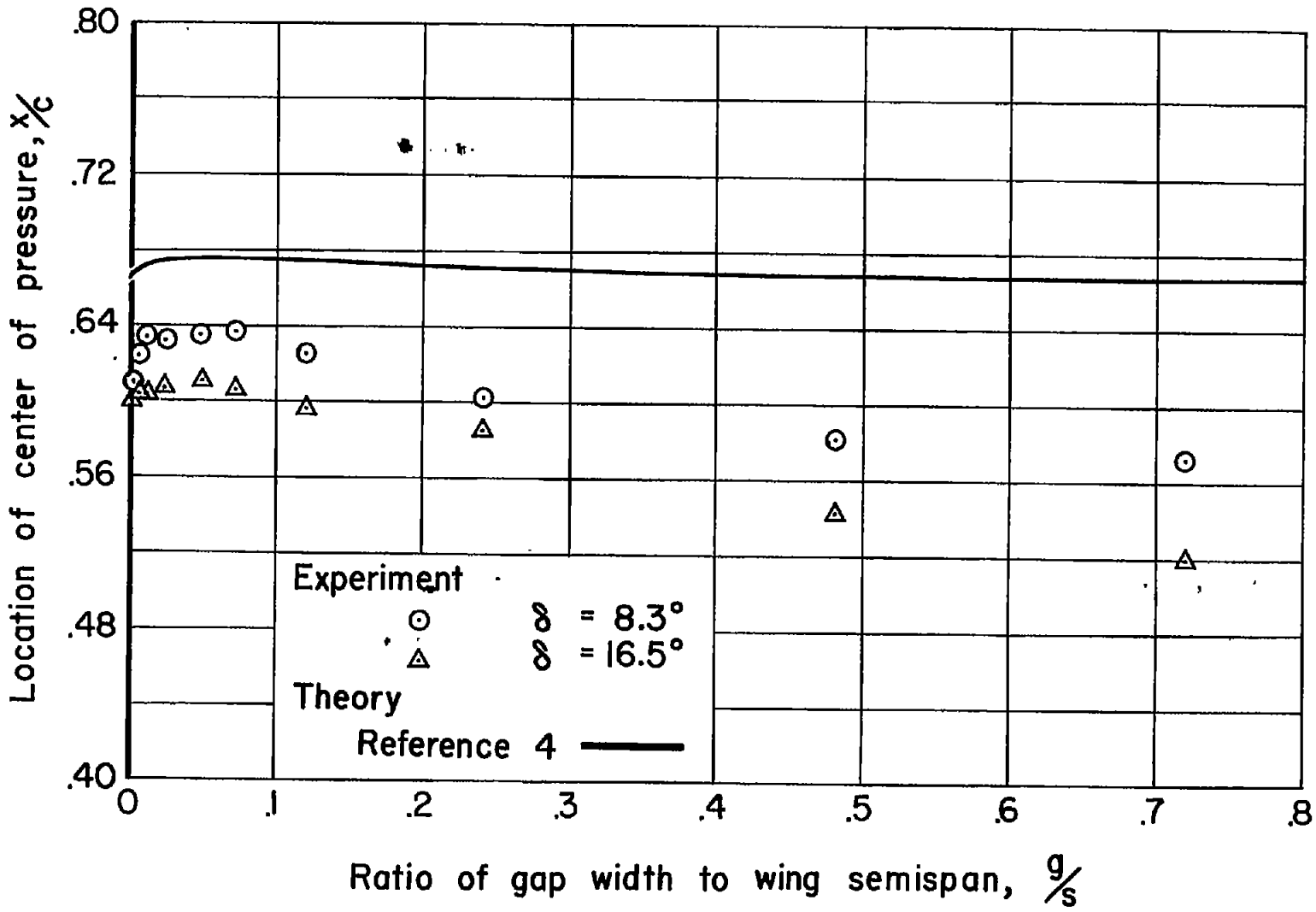

Figure 9.- Effect of gap upon streamwise location of center of pressure of deflected wing; $\alpha = 0$.

symbol	⊙	⊡	◇	△	◺	◺	⌂	◇	◇	⌂
gap, in.	.010	.050	.100	.200	.400	.600	1.00	2.00	4.00	6.00
$\frac{\text{gap}}{\text{semispan}}$	.0012	.006	.012	.024	.048	.072	.120	.240	.481	.721

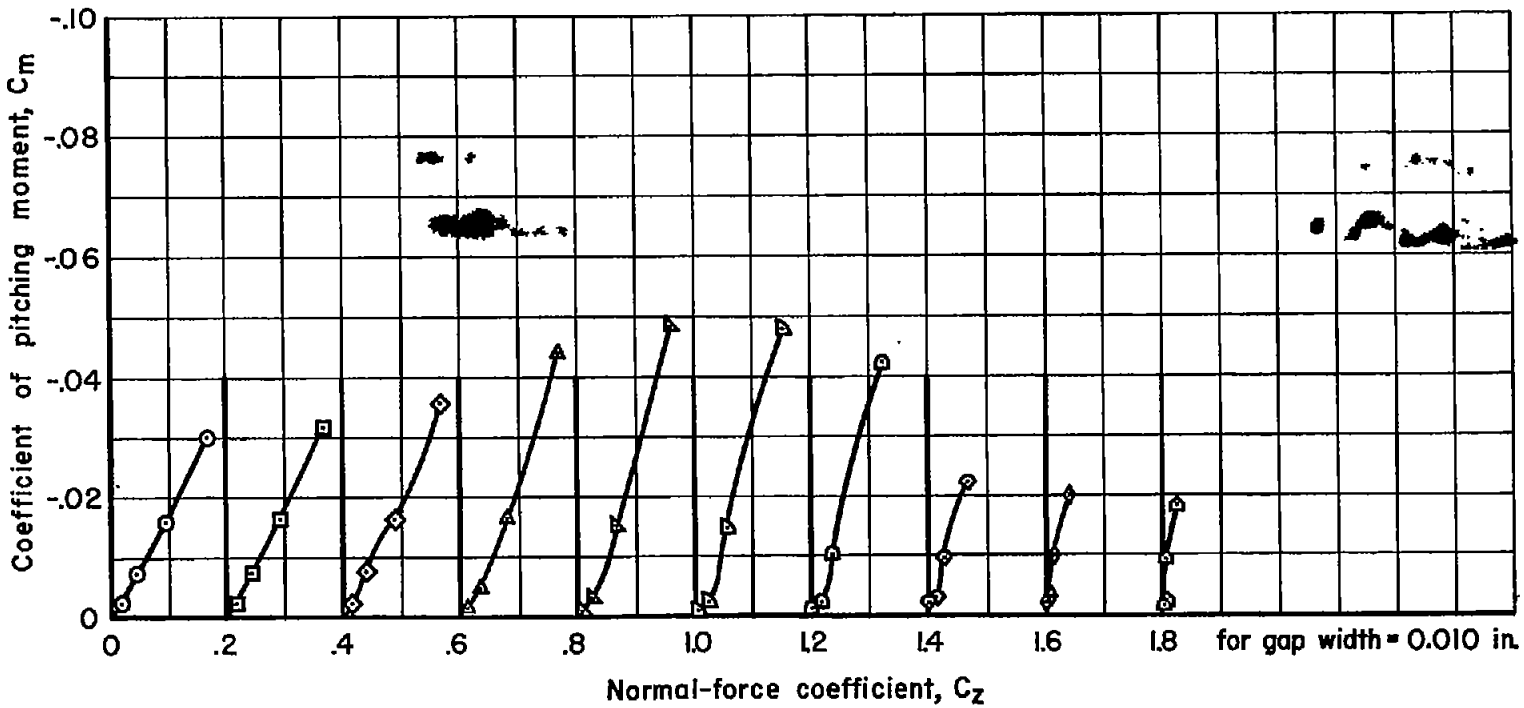

Figure 10.- Effect of gap upon variation of pitching moment of body with body normal force, $\alpha = 0$ (nose and afterbody included).